AAPS PharmSciTech (2021) 22: 79
DOI: 10.1208/s12249-021-01945-8

Research Article

Theme: Pharmaceutical Thermal Processing - An Update
Guest Editors: Feng Zhang, Michael Repka and Suresh Bandari

A One-Step Twin-Screw Melt Granulation with Gelucire 48/16 and Surface Adsorbent to Improve the Solubility of Poorly Soluble Drugs: Effect of Formulation Variables on Dissolution and Stability

Sandeep Sarabu,[1] Venkata Raman Kallakunta,[1] Arun Butreddy,[1] Karthik Yadav Janga,[1] Srinivas Ajjarapu,[1] Suresh Bandari,[1] Feng Zhang,[2] S. Narasimha Murthy,[1] and Michael A. Repka[1,3,4]

Received 13 October 2020; accepted 26 January 2021; published online 19 February 2021

Abstract. Fenofibrate is an effective lipid-lowering drug; however, its poor solubility and high log *p* (5.2) result in insufficient absorption from the gastrointestinal tract, leading to poor bioavailability. In this study, a one-step continuous twin-screw melt granulation process was investigated to improve the solubility and dissolution of fenofibrate using Gelucire® 48/16 and Neusilin® US2 as the solubilizer and surface adsorbent, respectively. The formulations (granules) were prepared at different ratios of fenofibrate, Gelucire® 48/16, and Neusilin® US2 based on phase-solubility studies and characterized using dissolution, differential scanning calorimetry, powder X-ray diffraction, and scanning electron microscopy analyses and studies on flow properties. In the phase-solubility studies, a linear relation was observed between Gelucire® 48/16 concentration and the amount of fenofibrate dissolved. In contrast, the dissolution rate of the prepared formulations was independent of the fenofibrate: Gelucire® 48/16 ratio and dependent on the Neusilin® US2 levels in the formulation. Increasing Neusilin® US2 levels decreased the rate of dissolution of the granules but improved the stability of the tablets under storage at accelerated stability conditions. Interestingly, higher Gelucire® 48/16 levels in the granules resulted in tablets with a hard matrix, which slowed disintegration and dissolution. All formulations exhibited improved dissolution compared to pure fenofibrate.

KEY WORDS: twin-screw melt granulation; gelucire® 48/16; neusilin US2; solubility enhancement; fenofibrate; compressibility; dissolution rate

INTRODUCTION

Poor drug bioavailability is a major and common challenge in the process of oral drug product development. It could result from factors such as low aqueous solubility, slow dissolution rate, poor drug permeability, and high first-pass metabolism (1). However, among these, poor solubility has been the most frequent cause of poor bioavailability (2); more than 40% of new chemical entities developed in the pharmaceutical industry exhibit poor aqueous solubility (3). Several techniques are used to improve drug solubility, including particle-size reduction (4), co-crystallization, co-amorphization, salt formation, cyclodextrin complexation, surfactants, solid dispersions (SDs), and lipid-based drug delivery systems (LBDD) (5–10).

The last decade has seen increased interest in lipids as carriers for the delivery of poorly soluble drugs (11) because of their acceptable regulatory and safety profiles and ability to enhance oral bioavailability. Various systems, including liquid/solid solutions, SDs (12), self-microemulsifying/self-nanoemulsifying drug delivery systems (13), and lipid nanoparticles, such as solid lipid nanoparticles and nanostructured lipid carriers (14), have been successfully prepared using lipids as drug carriers. Despite the aforementioned advantages associated with lipids, certain factors, such as poor stability and difficulty in manipulation (pulverization) associated with their low melting temperatures, have limited their application in the development of solid dosage forms (15). Considering the physical nature (liquid or semi-solid) of most lipids, liquid-filled capsules (hard and soft gelatin) are the most preferred dosage choice for a lipid-based formulation. However, factors like interaction with fill materials and material leakage are some of the problems associated with liquid-filled capsules (16, 17). To counter these challenges,

[1] Department of Pharmaceutics and Drug Delivery, The University of Mississippi, University, Mississippi 38677, USA.
[2] College of Pharmacy, The University of Texas at Austin, Austin, Texas 78712, USA.
[3] Pii Center for Pharmaceutical Technology, The University of Mississippi, University, Mississippi 38677, USA.
[4] To whom correspondence should be addressed. (e–mail: marepka@olemiss.edu)

lyophilization, melt granulation, and spray drying techniques (18–21) have been widely used to transform LBDDs into either tablets or capsules. Recently, hot-melt extrusion (HME), a continuous manufacturing technique, was successfully used (22, 23) to prepare solid self-emulsifying drug delivery systems (S-SEDDS). Silva *et al*., for the first time, reported the application of HME to transform conventionally prepared liquid self-emulsifying drug delivery systems (L-SEDDS) into an S-SEDDS by blending with solid carriers hydroxypropyl methylcellulose acetate succinate (HPMCAS) and microcrystalline cellulose (22). The addition of HPMCAS prevented the reconstitution of microemulsions and also retarded the drug release in gastric conditions.

Melt granulation is achieved by the addition of either a molten or solid binder that melts during the process. The advantages of melt granulation are that it is a solvent-free process and has improved tabletability compared to conventional wet and dry granulation processes (24, 25). Another commonly used approach to solidify a lipid-based formulation is adsorbing them on to porous carriers such as silicates. This combination of lipid formulations and adsorbents with high specific surface area has been used in the preparation of immediate-release formulations of various drugs (12, 18, 26). Neusilin® (NEU), a synthetic magnesium aluminometasilicate, is one such porous carrier with suitable flowability (18), superior compressibility (27), and large specific surface area. It also exhibits high oil- and water-adsorbing capacity (28, 29). Additionally, NEU helps in the stabilization of moisture-sensitive and lipophilic drugs. NEU is available in different grades, which differ in their bulk densities, particle size, and pH (30). NEU as a solid carrier was used in a variety of process techniques that included co-grinding, twin-screw extrusion, high shear granulation, and spray drying. It is one of the explored solid carriers for self-emulsifying drug delivery systems. The combination of well-defined pore systems and high surface area makes NEU a potential carrier for therapeutic molecules (31, 32). NEU UFL2 grade was successfully used to improve the solubility and bioavailability of fenofibrate (FEN). FEN was loaded on to UFL2 by a melt-adsorption method using supercritical carbon dioxide. Application of supercritical fluid facilitated the introduction of the active in to the pores of NEU UFL2 (33). NEU US2 (US2) grade has been reported in the preparation of liquid-solid compacts (34), transforming liquid SEDDS into solid SEDDS containing several drugs (13, 21, 35, 36). It has also been used as a carrier to stabilize the amorphous states of drugs, such as ketoprofen, indomethacin, naproxen, and progesterone (37) via HME and co-grinding (38, 39). NEU US2 was used along with Gelucire® (GEL) in hot-melt granulation (12) to improve the solubility and bulk properties of the poorly water-soluble drug, BAY 12-9566. Gelucires are amphiphilic surfactants. Chemically, they are polyethylene glycol (PEG) esters with a hydrophilic PEG portion and a lipophilic fatty acid portion (40). They are available in a wide range of HLB values and are often used to improve the solubility and bioavailability of poorly soluble drugs (41) and in preparation of floating (42, 43) and sustained release (44) dosage forms. Due to their low melting temperatures (<65°C), they are highly suitable for melt granulation processes.

Conventional hot-melt granulation using Gelucire® is a batch process that involves multiple steps. First, the drug is solubilized in molten Gelucire® maintained at a temperature to obtain a clear molten mixture. Later, the clear molten mixture is added dropwise to a preheated surface adsorbent in a granulator to obtain ternary dispersion granules (12). To the best of our knowledge, this is the first study to attempt to overcome this problem, and we investigated a single step twin-screw melt granulation (TSMG) process involving simultaneous dispersion and adsorption to enhance the dissolution of poorly soluble fenofibrate (FEN) as the model drug, using Gelucire® 48/16 (GEL) and US2 as the SD carrier and surface adsorbent, respectively. GEL is a non-ionic solid surfactant. Chemically, it is a polyethylene glycol ester of fatty acid. It has a high hydrophilic-lipophilic balance of 12, which makes it a suitable carrier for poorly soluble drugs. Further, we evaluated the effect of the GEL and US2 levels on dissolution, bulk properties of the granules, stability, and drug release from the prepared tablets.

MATERIALS AND METHODS

Materials

FEN was kindly donated by Ashland Inc. (Ashland Inc., Lexington, KY, USA), and GEL was gifted by Gattefosse (NJ, USA). NEU US2 and S2 were donated by Fuji Chemical Industries USA, Inc. (NJ, USA). The diluent Avicel® PH 102 and superdisintegrant Ac-Di-Sol® were gifted by FMC Biopolymer (PA, USA); magnesium stearate (MS) was gifted by Peter Greven Corporation (NJ, USA). All the other chemicals used in the study were of analytical grade.

Preformulation

Phase-Solubility Studies

Solubility studies for FEN were performed in aqueous solutions of GEL (0–12 mM). An excess amount of drug was added to 10 mL of each aqueous solution, and the solutions were incubated in an orbital shaker (Taitec Bioshaker, Saitamaken, Japan) for 48 h at 100 rpm and 25°C. Subsequently, the samples were centrifuged at 13,000 rpm for 15 min, and the supernatant was filtered (0.45 μm PVDF) and diluted with the respective media for quantification of the drug using high-performance liquid chromatography (HPLC). All tests were performed in triplicate. The apparent stability constant (K_c) was calculated from the slope of the phase-solubility diagrams using the following equation (45):

$$K_c = \frac{\text{Slope}}{S_0(1-\text{slope})} \quad (1)$$

The slope was obtained from the straight-line portion of the plot of FEN concentration against GEL concentration, and S_0 is the solubility of FEN in water, in the absence of GEL.

HPLC

The concentration of FEN in the dissolution samples was quantified using an HPLC system (Waters Corp, Milford,

MA, USA). The HPLC method stated in USP-NF was adopted (46); a Phenomenex Luna® C18 reverse phase column (5 μm, 100 Å, 250×4.6 mm) was used as the stationary phase. The mobile phase consisted of acetonitrile and acidified water (70:30); the water was adjusted to pH 2.5 ±0.1 using phosphoric acid as acidified water. The flow rate was maintained at 1.2 mL/min, and the UV-detector was set at 286 nm (Waters 2489 UV/detector). Ten microliters of the sample was injected, and the data were analyzed using the Empower 3 software. A six-point calibration curve was plotted and found to be linear in the concentration range of 2–50 μg/mL with a correlation coefficient (R^2) of 0.999.

Thermal Analysis

Differential Scanning Calorimetry (DSC). DSC was performed to determine the melting temperatures of FEN and GEL using Discovery DSC 25 (TA Instruments DSC, New Castle, DE, USA), coupled with an RCS90 cooling device. The instrument was calibrated for temperature and heat capacity using indium and sapphire standards. Samples weighing approximately 10 mg were sealed in a Tzero aluminum pan. The samples were equilibrated under nitrogen gas for 1min at 25°C and subsequently heated at 10°C/min from 25 to 200°C under an inert nitrogen purge of 50 mL/min. The thermograms were analyzed to detect the melting temperature.

Selection of Surface Adsorbent for the TSMG Process

Screening studies were performed to select the adsorbent NEU (US2 and S2) and CEOLUS™ (UF–711 and UF-702) grades. Surface adsorbents enhance the processability of a product by improving its flow and compressibility (12, 47). CEOLUS™ is microcrystalline cellulose and is available in three different powder grades, UF, KG, and PH (48, 49). These grades can impart characteristics such as compactability, disintegration, and flow to the formulation due to their highly porous morphology.

Cryomilled GEL sieved through USTM #25 was used in the granulation experiments. Physical mixtures prepared at 1:2:0 and 1:2:1 (FEN:GEL:surface adsorbent) ratios were processed through a 16-mm (ThermoScientific® Prism Eurolab) extruder with a standard screw configuration consisting of three mixing zones at 100 rpm speed and 100°C processing temperature. The surface adsorbent was selected based on the appearance and flow properties of the product obtained in these experiments. The flow properties were assessed by evaluation of angle of repose as per the methods previously reported (50, 51).

Twin-Screw Granulation

Twin-screw granulation was performed using the Thermofischer standard screw configuration consisting of three mixing zones. Two different process temperatures (60°C and 100°C) were evaluated for the melt granulation process, with a constant screw speed of 100 rpm. After initial screening studies, six formulations (F1 to F6) were prepared at different drug:solubilizer:adsorbent ratios, as shown in Table I. Granulation was performed on a 16-mm (ThermoScientific® Prism Eurolab) extruder with a screw speed of 100 rpm and at a process temperature of 100°C. The feed rate was maintained constant between 3.5 and 4.0 g/min. The obtained granules were milled using a kitchen blender; those that passed through ASTM #25 were collected and used in further studies.

Evaluation of Particle-Size Distribution (PSD)

PSD was determined for the granules obtained in the twin-screw granulation by sieve analysis using a vibratory sieve shaker (Performer III SS-3, Gilson Inc., OH, USA). The analysis was conducted using a pre-weighed sieve nest combination of #20, 30, 40, 60, 80, 120, and 200 ASTM mesh series. An accurately weighed quantity (10 g) of the sample was discharged into the sieve nest, and the analysis was conducted for 10 min at an amplitude of 5 with a tapping rate of 60 taps/min. The retained amount of powder on each sieve was accurately weighed after the analysis. PSD plots were generated on the basis of the weight distribution on each sieve.

Solid-State Characterization

DSC and Powder X-Ray Diffraction Measurement (PXRD)

DSC studies were performed for the physical mixtures and granules using Discovery DSC 25 (TA Instruments DSC, New Castle, DE, USA), coupled with a RCS90 cooling device. All samples weighed approximately 5–10 mg; they were sealed in a Tzero aluminum pan. The samples were equilibrated for 1 min at 25°C and subsequently heated at 10°C/min from 25 to 125°C under an inert nitrogen purge of 50 mL/min. The thermograms were analyzed to determine the amorphous or crystalline nature of the drug.

PXRD studies were performed for FEN and granules using the Rigaku X-ray system (D/MAX-2500PC, Rigaku Corporation, Tokyo, Japan) equipped with a copper tube anode and standard sample holder. Diffraction measurements were performed under the following conditions: CuKα radiation, 40 kV voltage, and 40 mA current. The 2θ scanning range was 2–50° with a step width of 0.02 °/S at a scanning speed of 2 °/min. Samples placed on a sample holder were gently compressed with a clean metal bar, and diffractograms were collected at room temperature (20–25°C).

Fourier Transform Infrared Spectroscopy (FTIR)

FTIR studies were performed on an Agilent Cary 660 FTIR Spectrometer (Agilent Technologies, Santa Clara, CA, USA). To study the interaction between the drug and formulation components, a small amount of sample placed on top of a diamond crystal was pressed with a MIRacle high-pressure clamp, and the spectrum was collected over 600–4000 cm^{-1} with 16 scans at a resolution of 4 cm^{-1}. The FTIR bench was equipped with an attenuated total reflection (Pike Technologies, Madison, WI, USA), which was fitted with a single-bounce, diamond-coated ZnSe internal reflection element.

Table I. Formulation Composition and Torque Values Observed in the Granulation Process

Formulation	Fenofibrate (%w/w)	Gelucire 48/16 (%w/w)	Neusilin US2 (%w/w)	Ratio FEN:GEL: NEU	Torque (Nm)	Molten portion to adsorbent ratio
F1	33.33	33.33	33.33	1:1:1	0.152	2.00
F2	25.00	37.50	37.50	1:1.5:1.5	0.158	1.67
F3	20.00	40.00	40.00	1:2:2	0.160	1.50
F4	25.00	25.00	50.00	1:1:2	0.157	1.00
F5	25.00	50.00	25.00	1:2:1	0.155	3.00
F6	25.00	0.00	75.00	1:0:3	0.162	0.33

Scanning Electron Microscopy (SEM)

The surface morphology of FEN, cryomilled GEL, US2, physical mixtures, and formulations were assessed using a JSM-7200FLV Field-Emission Scanning Electron Microscope (JEOL, Peabody, MA, USA) with an accelerating voltage of 5 kV. All samples were placed on the SEM stubs and adhered using double adhesive tape. The samples were sputter-coated with platinum under an argon atmosphere using a fully automated Denton Desk V TSC Sputter Coater (Denton Vacuum, Moorestown, NJ, USA) prior to imaging.

Dissolution Studies of Granules

In vitro drug-release studies for pure FEN and FEN formulations were performed with a dose equivalent to 50 mg FEN filled in capsules in 1000 mL of water at different concentrations (0.005, 0.01, and 0.025 M) of surfactant (sodium lauryl sulfate (SLS)) as a release media, using USP apparatus type II (SR8-plus™, Hanson, CA, USA) maintained at 37±0.5°C with a paddle speed of 50 rpm for 2 h (n=3). Sample aliquots (3 mL) were collected at 15, 30, 45, 60, 90, and 120 min and replaced with an equivalent volume of fresh media maintained at 37±0.5°C. The samples were filtered through a 0.45-μm PVDF membrane (Durapore®; Millpore Sigma, MA, USA) filter and quantified using HPLC (Waters Corp)**.**

Evaluation of Flow Properties and Tableting

For tablet preparation, Avicel® PH 102 (microcrystalline cellulose; MCC), Ac-Di-Sol (croscarmellose sodium), and MS were chosen as excipients. The flow properties of the formulations were evaluated before addition of the tableting excipients by measuring Carr's index (CI) (51). Five grams of each sample was placed in a 10-mL graduated cylinder, and the volume was recorded. The cylinder was tapped continuously on a flat surface until a constant volume was achieved or until the difference between two consecutive volume readings was less than 2.0%. The bulk and tapped densities were calculated from the weight and bulk and tapped volumes of the respective formulations. CI was calculated using Eq. (2), as follows:

$$CI = \left(\frac{D_T - D_B}{D_T}\right) \times 100 \tag{2}$$

where D_T is the tapped density, and D_B is the bulk density.

Tablets were prepared using a combination of (a) 250 mg of formulation and excipients and (b) different tablet weights but similar proportions (%w/w) of formulation and individual excipients (Table II). Tablets were compressed on a manual tablet compaction machine (MCTM I-GlobePharma, NJ, USA) using an 8-mm flat punch. Each tablet contained 50 mg equivalent of FEN. The compression force for the tablets was adjusted to maintain the breaking force at approximately 6–7 KP. The tensile strength (Q) of the tablets was determined using the following equation:

$$Q = \frac{2F}{\pi dt} \tag{3}$$

where F is the breaking force, T is the tablet thickness, and D is the diameter of tablet.

Physical Characteristics of the Tablets

The tablets were evaluated for weight variation, hardness, disintegration, and friability as per the procedures described in the United States Pharmacopeia and the National Formulary (USP-NF). Friability, breaking force, and disintegration were evaluated using FT2 friability (Schleuniger, Pharmatron, Thun, Switzerland), hardness (Optimal Inc, Michigan, USA), and disintegration testers (Schleuniger, Pharmatron, Thun, Switzerland), respectively. The dissolution of the tablets was compared with that of their respective granules in 0.025 M SLS.

Dissolution Data Analysis

The dissolution profiles were compared by model-independent methods; various dissolution parameters, such as dissolution efficiency (DE), initial dissolution rate (IDR), and mean dissolution rate (MDR), were calculated (52). The DE is calculated as the percentage ratio of the area under the dissolution curve up to a time, t, to that of the area of the rectangle described by 100% dissolution at the same time point. DE at 15, 30, and 60 min was calculated using the following Eq. (4):

$$\mathrm{DE} = \frac{\left(\int_0^t y \times dt\right)}{y_{100} \times t} \times 100\% \tag{4}$$

Table II. Tablet Composition

Tablet #	Granules taken (% w/w)	MCC (% w/w)	AcDiSol (% w/w)	Magnesium stearate (% w/w)	Tablet weight (mg)
T1 (F1)	60	34.5	5	0.5	250
T2 (F2)	80	14.5	5	0.5	250
T3 (F5)	80	14.5	5	0.5	250
T2_R*	60	34.5	5	0.5	333
T3_R*	60	34.5	5	0.5	333

**Reformulated T2 and T3 tablets, with formulation and excipients in same proportions as in T1*

IDR was calculated for the first 15min of dissolution using the following Eq. (5):

$$\mathrm{IDR} = \frac{\%\mathrm{dissolved}}{\mathrm{min}} \tag{5}$$

MDR was calculated using the following Eq. (6):

$$\mathrm{MDR} = \frac{\sum_{j=1}^{n} \Delta Mj/\Delta t}{n} \tag{6}$$

where j is the dissolution sample number, n is the number of dissolution sampling times, Δt is the time at midpoint between two consecutive time points (t_j and $t_{j\text{-}1}$), and ΔM_j is the additional amount of drug released between two consecutive time points (t_j and $t_{j\text{-}1}$).

Stability Studies

The prepared tablets were subjected to stability studies under accelerated stability conditions (40°C and 75% relative humidity (RH)) for 3 months. Samples collected from the stability chamber (Caron, 6030) after 1 and 3 months were observed for physical appearance and tested for amorphous/crystalline nature of the drug, drug content, and dissolution. The similarity factor (f_2) was calculated using the following Eq. (7):

$$f2 = 50 \log\left\{\left(1 + \left(\frac{1}{n}\right)\sum_{t=1-n}(R_t - T_t)^2\right)^{0.5} \times 100\right\} \tag{7}$$

where R_t is the cumulative drug release of initial samples, T_t is the cumulative release of test sample at predetermined time points, and N is the number of time points.

The f_2 value ranges from 1 to 100: the higher the f_2 value, the higher the similarity. An f_2 value greater than 50 is considered similar.

Statistical Analysis

The statistical analysis of the *in vitro* drug release profiles was performed using the GraphPad Prism software (Version 5.0, GraphPad Software Inc., La Jolla, CA, USA). One-way ANOVA followed by Tukey's multiple comparison test was performed to compare the drug release profiles of different formulations. For values of $p < 0.05$, differences were considered statistically significant.

RESULTS AND DISCUSSION

Preformulation Results

Phase-Solubility and Thermal Analysis

The phase-solubility studies indicated that the apparent solubility of FEN increased linearly as a function of GEL concentration. The improvement of drug solubility could be attributed to the amphiphilic nature of GEL; improved wetting characteristics and micellar solubilization are two possible mechanisms (53, 54) for improved solubility of FEN. The solubility increased by approximately 73-fold in the 2% GEL solution (142.34 ± 2.2 mg/L) compared to its solubility in water (1.94 ± 0.12 mg/L). K_c was calculated as 6 mM^{-1} from the linear plot of the phase-solubility diagram. Higuchi and Connors defined this type of linear relation as A_L phase diagram (45).

DSC

The sharp endothermic peaks at 82.40°C and 48.15°C correspond to the melting peaks of FEN and GEL, respectively. These values were in agreement with those reported by previous studies (52, 55). The low melting point of GEL makes it a suitable carrier for melt granulation and extrusion.

Screening of Adsorbent Carrier

Among the different adsorbents that were screened, melt granulation of GEL with NEU US2 grade resulted in granules with suitable flow properties (angle of repose: 34°), whereas NEU S2 and Ceolus grades formed a waxy material, which on cooling turned into large chunks and hard cake, respectively. The difference in the flow properties and appearance of the product could be attributed to their differences in adsorbing capacity due to the difference in particle size, pore size, pore volume, surface functionality, specific surface area values, etc. (56). Silica grades exhibit better adsorbing capacity than MCC (57). Therefore, the US2 grade was selected as the adsorbent for the twin-screw granulation process. In the formulations without an adsorbent, the product existed as a semi-solid that turned to a waxy solid upon cooling.

Twin-Screw Granulation

Process temperatures of 60°C and 100°C were studied for formulations (F1 to F3). Similar torque values were observed at both processing temperatures (0.155–0.167 Nm). The formulations prepared at 100°C did not exhibit any thermal events at the melting temperature of FEN, whereas an endothermic peak at the melting temperature of FEN was observed in formulations prepared at 60°C, indicating the crystalline nature of the drug (data not shown).

These events suggest the significance of processing temperature on physical state of API in TSMG. Therefore, a 100°C process temperature and 100 rpm screw speed were used in the granulation process to ensure efficient mixing between GEL and FEN and simultaneous adsorption on to US2. The process torque values were low (0.155–0.167 Nm) and similar for all the formulations; however, a significant difference was observed in the appearance and physical properties (density and PSD) of the formulations. GEL in molten form additionally acts as a binder; it is responsible for granule formation. Coarser granules were formed with formulations F1 and F5; they required milling and sieving, whereas F2, F3, F4, and F6 exhibited the desired size and required only sieving for downstream processing.

PSD

The PSD data (Fig. 1) indicated that the granule size of the formulations was influenced by the US2 levels in the formulations. The particle size of formulations F1 and F5 was greater than 850 μm, whereas the fraction of granules above 250 μm in formulations F2 and F3 was approximately 51% and 27%, respectively. This might be due to the saturation of pores of US2 in the case of F1 and F5, which led to the deposition of excessive material on the surface of US2, thereby increasing the granule size. However, a major proportion of granules in formulations F4 and F6 were less than 180 μm (61.8% and 92.6%, respectively). The granule growth (size) was also dependent on the ratio of molten components to adsorbent of the formulations. The higher the proportion of molten components in the formulation, the larger is the granule size. An increase in GEL concentration with a simultaneous decrease in US2 levels promoted granulation. The levels of GEL and US2 and the ratio of molten components to adsorbent are displayed in Table I.

Solid-State Characterization

DSC and PXRD

DSC studies were performed to determine the physical state of the drug in the physical mixtures and the prepared formulations. In the F1 physical mixture, endothermic peaks were observed at 45.07°C and 82.09°C, which corresponded to the melting point of GEL and FEN, respectively. Whereas in the F6 physical mixture, a single endotherm at 81°C corresponds to the melting temperature of FEN; however, the intensity is greatly reduced in the F6 physical mixture. This could be attributed to the lower drug load (25% w/w) in F6 PM compared to the F1 PM (33% w/w). For granules, the endotherm at 42°C corresponded to the melting temperature of GEL, and the low intense endotherms between 65 and 70°C corresponded to the melting suppression of FEN (Fig. 2a), indicating the miscibility between GEL and FEN (58). The enthalpy values for the formulations are significantly lower (1.3 to 5.0) compared to the 86.02J/g of pure FEN. However, no endothermic peak was identified in the F6 granules, confirming the amorphous conversion of the drug in the formulation. Moreover, the depression in melting point was greater in formulations with higher GEL concentration.

In the PXRD studies, crystalline FEN exhibited characteristic peaks at 12.1°, 14.5°, 16.9°, 21.0°, 22.4°, 24.2°, and 24.9° (Fig. 2b), whereas GEL exhibited peaks at 17.6°, 18.9°, and 22.9°. In the prepared formulations, peaks appeared at 23.07° and 19.09°, matching with the peaks for GEL. Additionally, several low intensity peaks appeared in formulations F1, F2, and F5, providing no conclusive evidence regarding the nature of the drug in these formulations. No characteristic peaks of crystalline FEN were observed in F6, confirming the amorphous nature of the drug.

The DSC and PXRD data indicate that there was a faint presence of crystalline FEN in the granule formulations F1, F2, and F5, while the drug was completely amorphous in the F6 formulation.

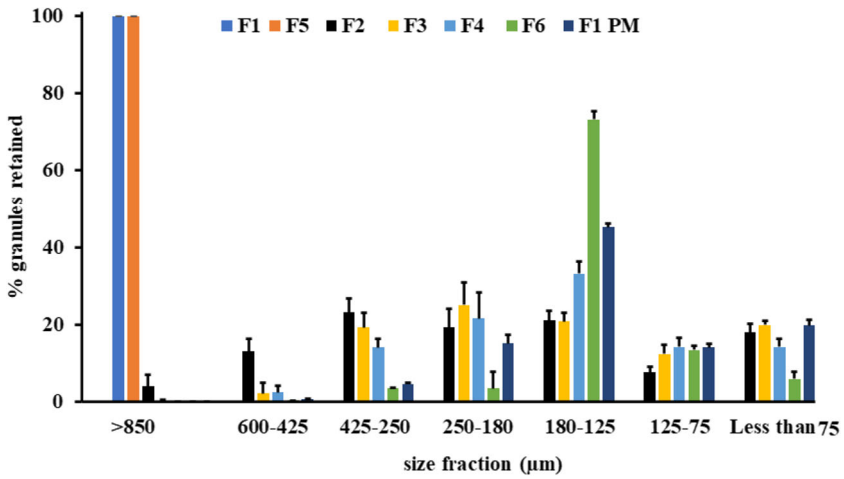

Fig. 1. Particle-size distribution in formulations F1–F6 and F1 physical mixture

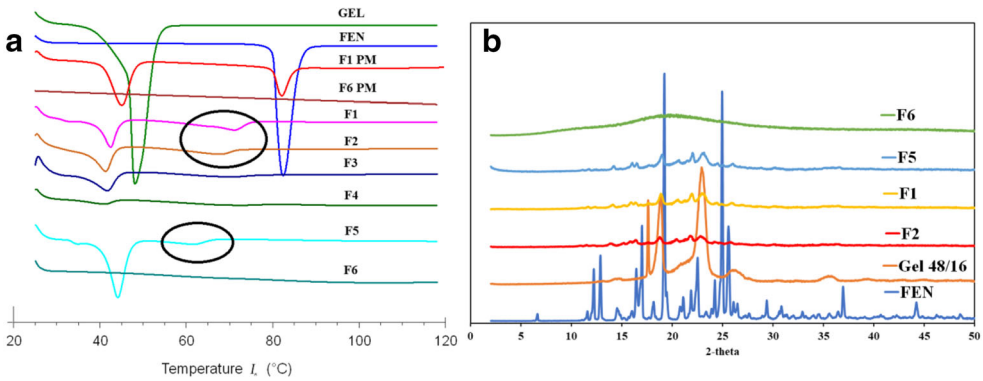

Fig. 2. **a** DSC thermograms of FEN drug, GEL, F1 and F6 physical mixtures and formulations (F1 to F6). **b** X-ray diffractogram of pure FEN, GEL, and formulations F1, F2, F5, and F6

FTIR

The FTIR spectra of FEN, GEL, US2, physical mixtures, and granule formulations are shown in Fig. 3. The FTIR analysis of pure FEN showed absorption at 1725 cm^{-1} for C=O stretching of the ester group, 1649 cm^{-1} for the C=O ketone group, and 2984 cm^{-1} for aromatic stretching (59, 60). The spectrum of GEL showed absorption bands at 2885, 1736, 1467, 1341, 1103, 959, and 842 cm^{-1} (61). US2 exhibited characteristic peaks at 3466 and 994 cm^{-1}. Similar peaks appeared in the physical mixtures and granule formulations (Fig. 3), indicating that FEN was compatible with GEL and US2. In formulations with lower levels of US2 (F1 and F5), an excess amount of GEL-FEN deposited on the surface of US2, promoting granule growth and intense peaks that were observed at wavenumbers corresponding to those of GEL and FEN in these granule formulations (Fig. 3).

In Vitro Drug Release Studies of Granules

In *in vitro* drug release studies of granules with water containing 0.025 M SLS as drug release media, there was an 8–10-fold increase in dissolution compared to pure FEN (Fig. 4a). Among all the formulations, F5 exhibited the highest IDR, followed by F1, F2, F3, F6, and F4; the percentage drug release at the end of 60 min (Q_{60}) followed the same order as IDR. F5 exhibited the highest and lowest DE and MDT values (Table III), respectively. The dissolution profiles of most formulations were similar (f_2 value greater than 50); however, the formulations exhibited different DE, MDT, and IDR values.

The dissolution and phase-solubility studies showed contrasting results. The dissolution studies indicated that the dissolution was dependent on the (a) US2 levels and (b) molten (FEN+GEL)-to-adsorbent proportions in the formulations rather than the ratio of FEN to GEL and drug load. This is illustrated in Fig. 4b and c; in formulations F1 to F3, the ratio of FEN:GEL increased from 1:1 to 1:2. However, the dissolution was higher with the F1 formulation (Fig. 4b). In the case of the F3 and F5 formulations, although both the formulations had the same FEN:GEL ratio (1:2), the drug release was significantly higher with the F5 formulation. This could be attributed to the lower US2 concentration (25% w/w vs. 40% w/w) and higher molten portion-adsorbent ratio in F5 (3:1) than in F3 (3:2).

Dissolution studies were further conducted in media with reduced SLS concentration (water + 0.01 M SLS and water +

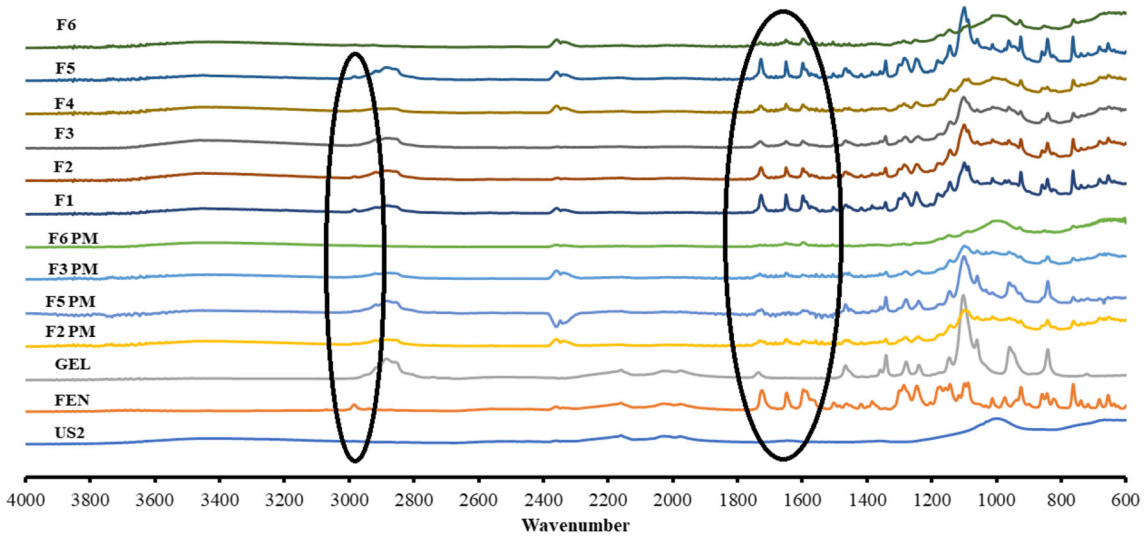

Fig. 3. FTIR spectra of pure FEN, GEL, physical mixtures, and formulations

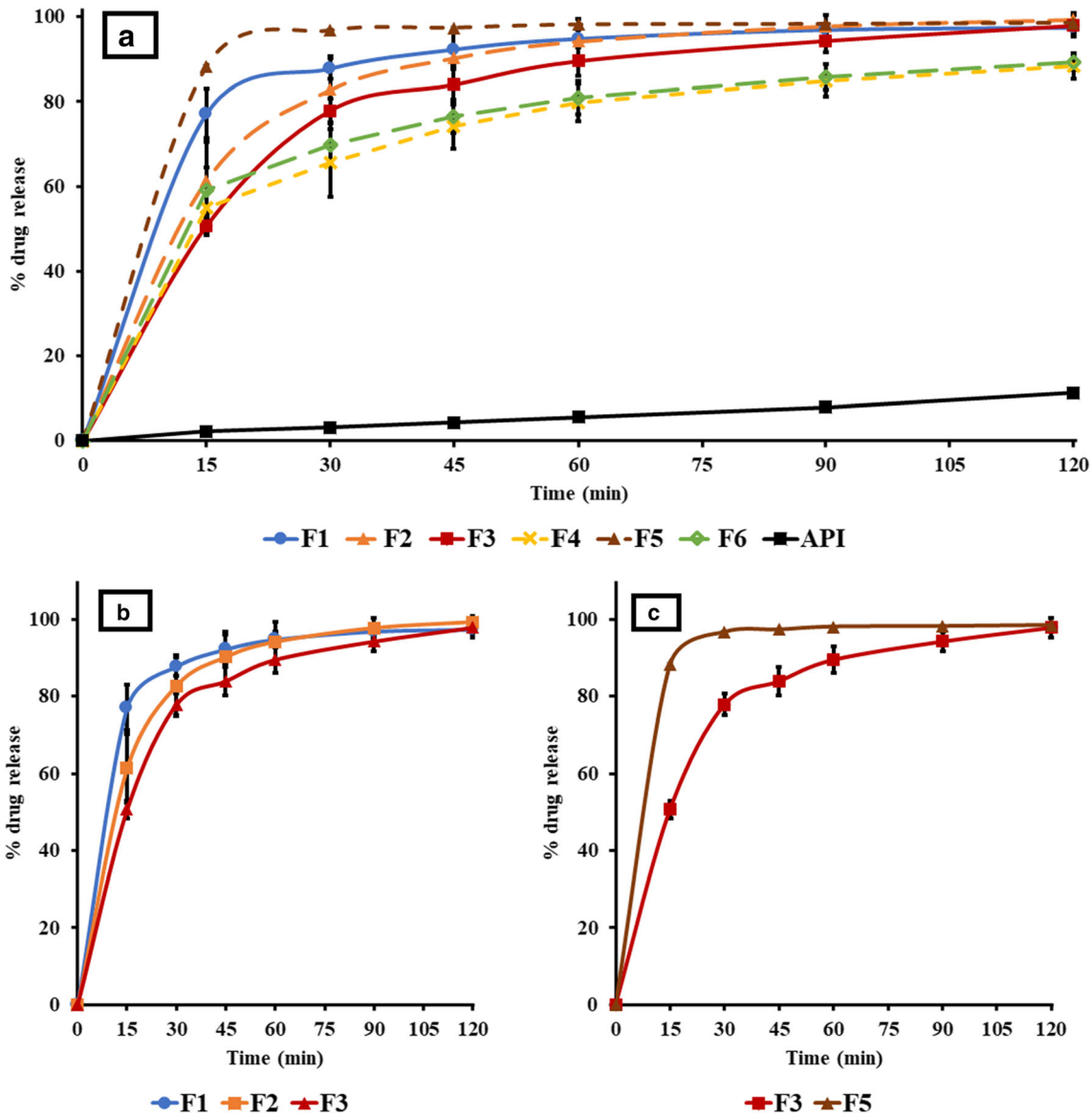

Fig. 4. Dissolution profiles of **a** pure drug FEN and formulations in water + 0.025M SLS, **b** formulations F1, F2, and F3, and **c** formulations F3 and F5

0.005 M SLS) to achieve discrimination. The drug release from formulations in 0.01 M SLS was higher than that with FEN drug; the dissolution trend (F5>F1>F2>F3>F6>F4) remained the same as that observed with a higher concentration of SLS in the dissolution media. However, the percentage dissolution decreased in water with 0.005 M SLS; a maximum drug release of 50% was achieved with the F5 formulation, whereas the other formulations showed a drug release of less than 30% (Fig. 5b). In 0.01 M SLS media, the percentage drug release was 94.80 ± 3.92, 88.00 ± 2.33, 85.50 ± 1.25, 76.50 ± 1.14, 67.70 ± 0.86, and 70.90 ± 1.43 at the end of 2 h of dissolution for the formulations F1, F2, F3, F4, F5, and F6, respectively (Fig. 5a). Discrimination was achieved between the F1, F2, and F5 formulations in 0.005 M SLS compared to 0.01 M and 0.025 M SLS. The f_2 values are tabulated in Supplementary Table ST1. A one-way ANOVA results indicated a statistically significant (p<0.05) difference in the dissolution profiles of formulations compared to FEN API in all of the dissolution media.

Formulations F1, F2 and F5 despite their relatively high crystallinity exhibited increased dissolution profiles compared to the less crystalline F3, F4, and F6. According to the dissolution profiles, the lower the levels of US2 in the formulation, the greater is the miscibility between FEN and GEL during the granulation process; therefore, the dissolution is greater. The US2 levels were in the following order: F5>F1>F2>F3>F4>F6. Hence, the dissolution trend followed the same order. Supplementary Figure S1 illustrates the Q_{15} value (percentage drug release after 15 min of dissolution in 0.025 M SLS) and PSD at different GEL, US2, and molten-to-adsorbent proportions.

Table III. Summary of Dissolution Parameters for FEN and Formulations (n=6); DE_{15}, DE_{30}, and DE_{60} Are Dissolution Efficiency Values at 15, 30, and 60 min; Q_{15} and Q_{60} Are the % Drug Released at 15 and 60 min; MDT, MDR, and IDR Are the Mean Dissolution Time, Mean Dissolution Rate, and Initial Dissolution Rate, Respectively

Media	Formulation Parameter	F1	F2	F3	F4	F5	F6	API
0.025M SLS in water	Q_{15}	77.1	61.33	50.64	54.88	88.2	59	2.21
	Q_{60}	94.79	94.15	89.5	79.76	98.08	80.94	5.52
	DE_{30}	59.73	51.36	44.78	43.81	68.27	46.96	1.88
	DE_{60}	75.37	70.34	64.3	58.58	82.81	61.46	3.09
	MDT	14.13	18.74	22.95	22.85	9.69	21.16	60.22
	MDR	1.82	1.65	1.39	1.37	2.03	1.45	0.08
	IDR	5.14	4.29	3.88	3.66	5.88	3.93	0.15
0.01M SLS in water	Q_{15}	56.39	47.74	44.11	37.62	81.49	39.15	1.06
	Q_{60}	77.92	72.82	66.78	57.38	92.11	58.96	2.45
	DE_{30}	44.42	38.58	35.84	30.52	62.63	31.53	0.91
	DE_{60}	52.63	46.61	43.44	36.94	71.44	38.01	1.179
	MDT	23.14	27.2	25.12	27.47	12.42	28.81	53.77
	MDR	1.39	1.22	1.13	0.97	1.88	1	0.03
	IDR	3.76	3.18	2.94	2.51	5.43	2.61	0.07
0.005M SLS in water	Q_{15}	11.1	9.44	7.55	9.59	16.07	12.06	0.07
	Q_{60}	31.87	28.23	24.4	18.98	51.39	23.31	0.23
	DE_{30}	10.82	9.31	8.01	8.67	16.03	10.49	0.067
	DE_{60}	15.12	13.19	11.68	11.21	23.12	13.55	0.096
	MDT	27.27	32.09	31.29	29.49	25.27	20.16	77.47
	MDR	0.37	0.32	0.27	0.28	0.55	0.33	0.0034
	IDR	0.74	0.63	0.5	0.64	1.07	0.8	0.0048

SEM

The SEM images of FEN exhibited crystals with a smooth surface; those of GEL were clustered with rough surfaces. US2 appeared as porous spherical particles. The SEM images of granules (Fig. 6) were consistent with the observations from the PSD studies. Granulation was significant in the F1 and F5 formulations; in the other formulations, the components were loosely bound. The morphology of the granules can influence mechanical properties, such as flowability and compressibility characteristics, which could be advantageous to the development of tablets. The concentration of US2 in the formulation significantly influenced granule-size distribution. Higher levels of adsorbent in the formulation offers greater surface area for adsorption, resulting in smaller granules; in contrast, at lower surfactant levels, FEN-GEL component was adsorbed in multiple layers, resulting in coarser granules.

Evaluation of Flow Properties and Tableting

Evaluation of the flow properties indicate that the granules obtained from the melt granulation of the F2 formulation and milling of F1 and F5 exhibit better

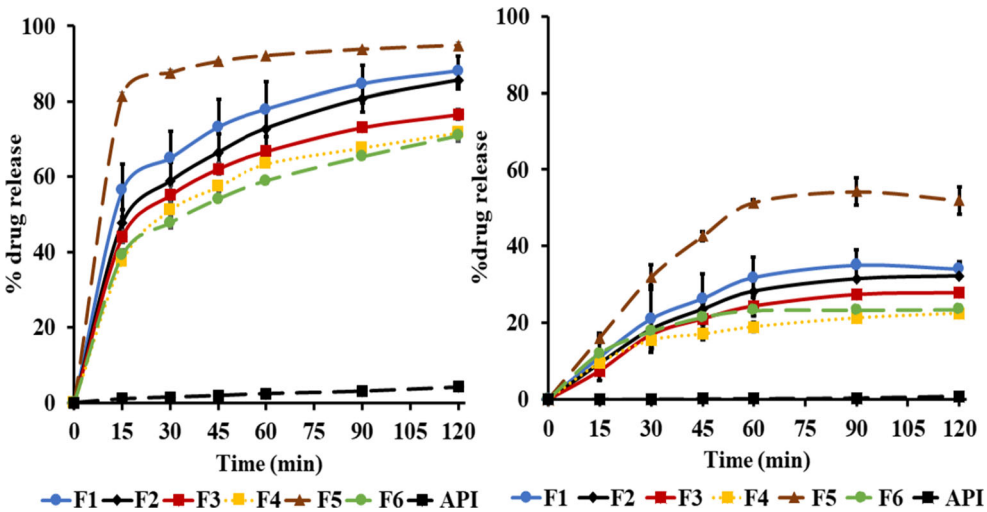

Fig. 5. Dissolution profiles of pure drug FEN and formulations in **a** water + 0.01 M SLS and **b** water + 0.005M SLS

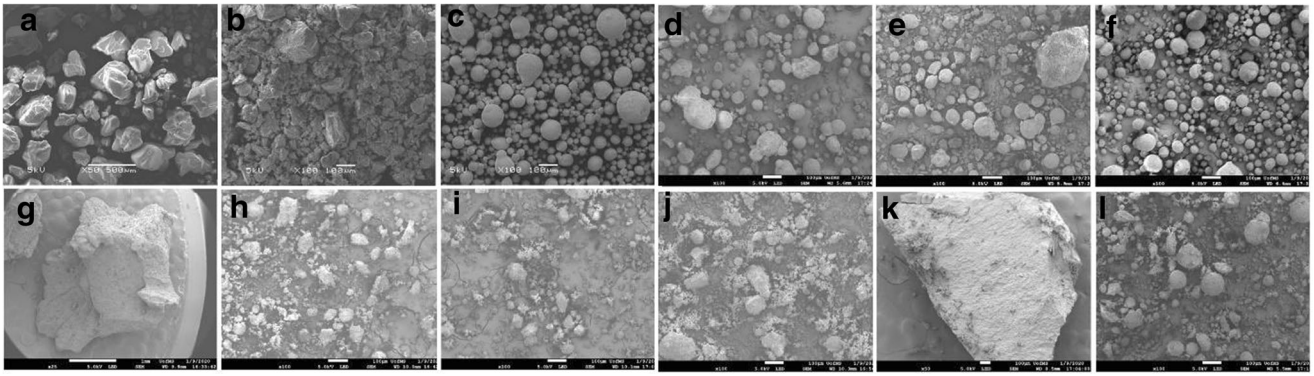

Fig. 6. SEM ×100 images of **a** FEN, **b** GEL, **c** NEU, **d** F2 PM, **e** F5 PM, **f** F6 PM, **g** F1, **h** F2, **i** F3, **j** F4, **k** F5, and **l** F6

compressibility (CI: 15–20, fair flow properties) than those obtained from F3, F4, and F6 (CI: 26-31, poor flow properties). Formulations F1, F2 and F5 also exhibited better dissolution properties compared to the F3, F4, and F6 formulations. Therefore, F1, F2 and F5 granules were further processed into tablets by blending granules with excipients (MCC, Ac-Di-Sol®), followed by compression and adjusting the compression force such that the hardness was 5–6 KP. The friability, hardness, disintegration, tensile strength, and assay values of the prepared tablets are provided in Table IV. The tensile strength of the tablets was greater than 1 Mpa (1.1 to 1.3); this ensures the mechanical strength of the tablets to withstand distribution (62, 63). T1 exhibits the fastest disintegration time compared to T2 and T3 possibly due to the higher extra granular proportion in T1. The prepared tablets were subjected to dissolution and stability studies.

In Vitro Dissolution Studies of Tablets

The dissolution profiles of the granules have been compared with those of their respective tablets to evaluate the influence of tableting on dissolution. T1 and F1 exhibited similar drug release profiles ($f_2 > 50$; 72.4), whereas T2 and T3 failed in showing similarity (Fig. 7) to their respective granules F2 and F5 ($f_2 < 50$).

Additionally, T2 and T3 exhibited higher disintegration time than T1 possibly due to the relatively lower extra granular proportion (20% w/w) in T2 and T3 than in T1 (40% w/w). The additional 20% extra granular proportion in T1 was constituted by MCC, which acts as a self-disintegrating agent. Moreover, it acts complimentary with super disintegrants to promote disintegration (64–66). On the basis of these results, T2 and T3 tablets were reformulated, increasing the extra granular proportion to 40% w/w as in tablet T1; the reformulated tablets of T2 and its corresponding granules (F2) showed similar dissolution (Fig. 8b) profiles ($f_2 > 50$; 82.4), whereas reformulated T3 failed to show similarity with F5 ($f_2 < 50$). Although F5 granules exhibited the best dissolution profile of all the six formulations, compression had decreased the dissolution rate possibly because the material deposited on the US2 surface in F5 granules had higher GEL (50% w/w) concentration; compression induces contact between the surface GEL particles and results in the formation of a hard matrix, which ultimately results in slower dissolution. This was additionally evidenced in the disintegration studies. The extra granular proportion significantly influenced the dissolution of tablets; increasing the extra granular proportion increased the dissolution rates.

Table IV. Tablet Physical Properties and Assay Results

Tablet #	% friability	Disintegration time (min)	Assay (%)
T1 (F1)	0.11±0.03	7.78±1.69	97.82±0.82
T2 (F2)	0.15±0.02	10.11±0.37	98.92±0.43
T3 (F5)	0.13±0.05	15.08±1.04	99.12±0.98
T2_R*	0.18±0.04	8.83±0.82	98.62±0.78
T3_R*	0.10±0.04	12.13±0.82	99.42±1.28

*R**, *Reformulated tablets*

Stability Studies

Tablets T1 and reformulated T2 were subjected to stability studies under accelerated storage conditions (40°C/75% RH). T2R tablet formulations were stable at 40°C and 75% RH for 3 months with respect to the amorphous nature of the drug and dissolution profile, as confirmed through DSC (Fig. 9) and dissolution studies. However, the T1 tablets exhibited slight recrystallization of FEN and appearance of an endothermic peak at approximately 80.5°C in the stability samples; additionally, the peak intensity increased in the 3rd month compared with the 1st month stability samples. The T1 tablets failed in the stability studies. The f_2 value for the T1 initial and T1 1M was less than 50, whereas the T2R tablets showed similar release profiles to that of initial samples even after 3 months of stability ($f_2 > 50$; 62.13), substantiating the similarity of the release profiles and stability of the samples. The failure of T1 in the stability studies could be attributed to the following factors: (a) phase separation of GEL and FEN during storage, as evidenced in DSC studies, (b) increase in disintegration time of the T1 stability samples, and (c) melting onset of GEL of approximately 38°C in formulations. Upon storage at 40°C, GEL softens and forms into a hard matrix, resulting in increased disintegration times, and it also resists the permeation of dissolution media into the tablet matrix. These changes were not observed in T2_R; the higher concentration of US2 provides sufficient surface area and prevents GEL recrystallization/phase separation. The drug content (%) values for T1 and T2 ranged from 98.9 ± 1.2 to 102.6 ± 0.9%, respectively.

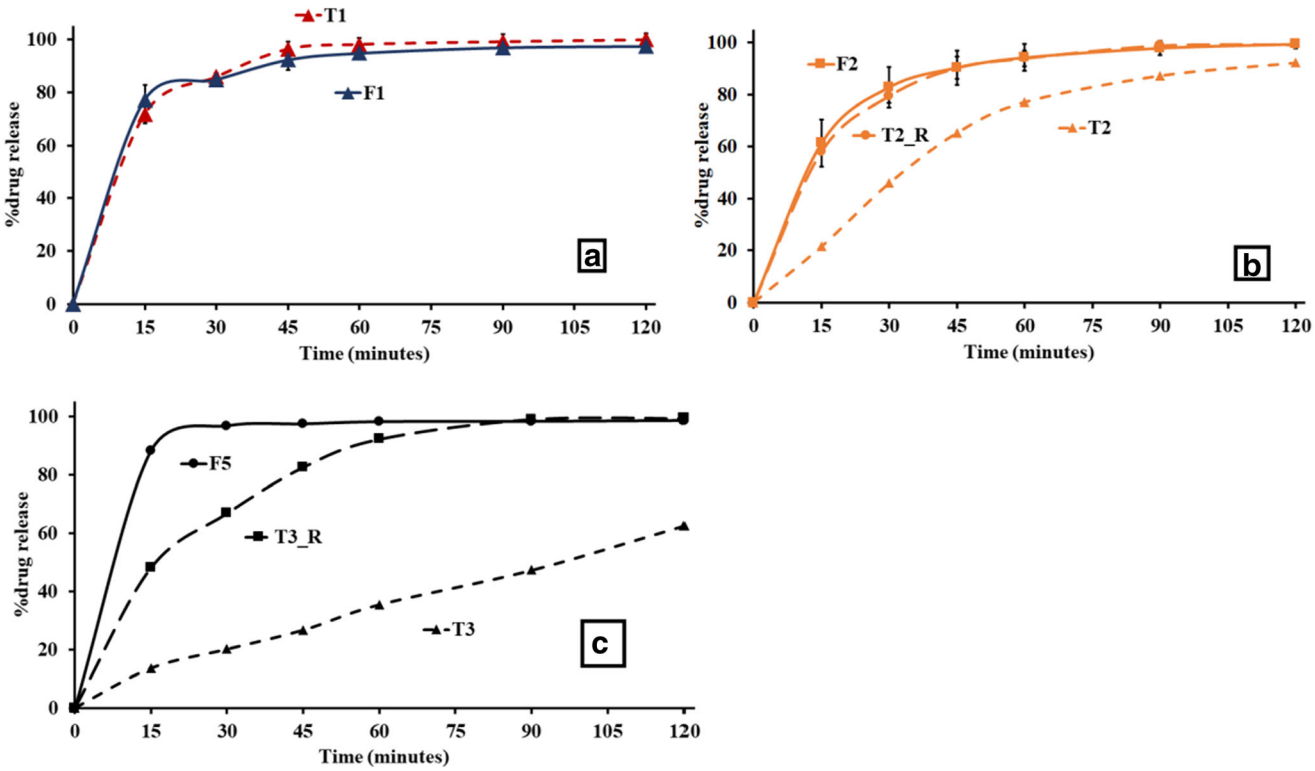

Fig. 7. *In vitro* drug release profiles of tablets (n=3): **a** F1 vs T1, **b** F2 vs T2 vs T2_R, and **c** F3 vs T3 vs T3_R

CONCLUSION

To the best of our knowledge, this is the first study to successfully investigate TSMG for the preparation of granules using GEL and US2 to improve the dissolution of FEN in a one-step process. The dissolution of FEN was enhanced in all the formulations compared to pure FEN. However, the rate and extent of dissolution were largely dependent on the concentration of US2 and molten portion-to-adsorbent ratio in the formulation. An increase in GEL concentration with a simultaneous decrease in US2 enhanced the granule growth, dissolution, and flow properties of the formulations (granules). In the compressed tablets, a higher GEL concentration (%w/w) decreased the dissolution rate; however, a higher US2 concentration (%w/w) improved the stability of the tablets, preventing recrystallization of FEN, as observed in the DSC studies. Twin-screw granulation using GEL and US2 is an easy and continuous process. However, systematic optimization of each component is required to produce a product with high dissolution rate and downstream capabilities.

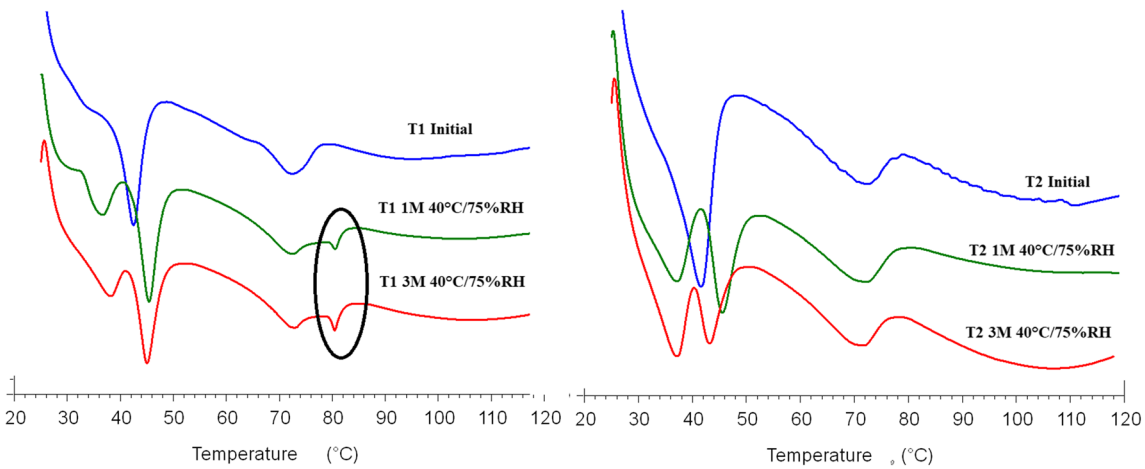

Fig. 8. DSC thermograms of T1 and T2 initial and stability samples

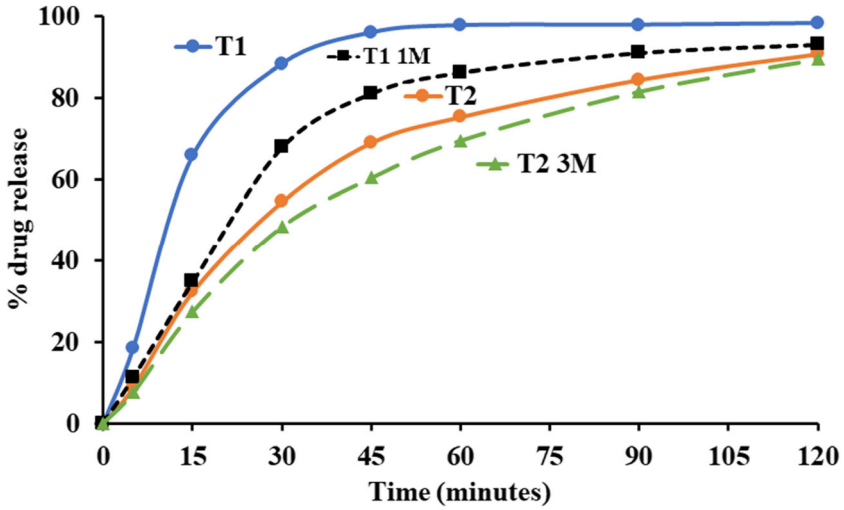

Fig. 9. *In vitro* dissolution profiles of T1 and T2 initial and stability samples

SUPPLEMENTARY INFORMATION

The online version contains supplementary material available at https://doi.org/10.1208/s12249-021-01945-8.

ACKNOWLEDGEMENTS

Scanning electron microscopy images presented in this work were generated using the instruments and services at the Microscopy and Imaging Center, The University of Mississippi. This facility is supported in part by grant 1726880, National Science Foundation.

FUNDING

This project was partially supported by Grant number P30GM122733-01A1, funded by the National Institute of General Medical Sciences (NIGMS), a component of the National Institutes of Health (NIH) as one of its Centers of Biomedical Research Excellence (COBRE).

REFERENCES

1. Jaipal A, Pandey MM, Charde SY, Sadhu N, Srinivas A, Prasad RG. Controlled release effervescent buccal discs of buspirone hydrochloride: in vitro and in vivo evaluation studies. Drug Deliv. Taylor & Francis. 2016;23:452–8.
2. Savjani KT, Gajjar AK, Savjani JK. Drug solubility: importance and enhancement techniques. ISRN Pharm. 2012;2012:1–10.
3. Lipinski C. Poor aqueous solubility—an industry wide problem in drug discovery. Am Pharm Rev. 2002;5:82–5.
4. Liversidge GG, Cundy KC. Particle size reduction for improvement of oral bioavailability of hydrophobic drugs: I. Absolute oral bioavailability of nanocrystalline danazol in beagle dogs. Int J Pharm. 1995;125:91–7.
5. Bookwala M, Thipsay P, Ross S, Zhang F, Bandari S, Repka MA. Preparation of a crystalline salt of indomethacin and tromethamine by hot melt extrusion technology. Eur J Pharm Biopharm. 2018;131:109–19.
6. Gursoy RN, Benita S. Self-emulsifying drug delivery systems (SEDDS) for improved oral delivery of lipophilic drugs. Biomed Pharmacother. 2004;58:173–82.
7. Loftsson T, Brewster ME, Masson M. Role of cyclodextrins in improving oral drug delivery. Am J Drug Deliv. 2004;2:261–75.
8. Mendonsa N, Almutairy B, Kallakunta VR, Sarabu S, Thipsay P, Bandari S, et al. Manufacturing strategies to develop amorphous solid dispersions: an overview. J Drug Deliv Sci Technol. 2019;55:101459.
9. Mu H, Holm R, Müllertz A. Lipid-based formulations for oral administration of poorly water-soluble drugs. Int J Pharm. 2013;453:215–24.
10. Sarabu S, Bandari S, Kallakunta VR, Tiwari R, Patil H, Repka MA. An update on the contribution of hot-melt extrusion technology to novel drug delivery in the twenty-first century: part II. Expert Opin Drug Deliv. 2019;16:567–82.
11. Pouton CW. Formulation of poorly water-soluble drugs for oral administration: physicochemical and physiological issues and the lipid formulation classification system. Eur J Pharm Sci. 2006;29:278–87.
12. Gupta MK, Goldman D, Bogner RH, Tseng Y-C. Enhanced drug dissolution and bulk properties of solid dispersions granulated with a surface adsorbent. Pharm Dev Technol. 2001;6:563–72.
13. Kallakunta VR, Bandari S, Jukanti R, Veerareddy PR. Oral self emulsifying powder of lercanidipine hydrochloride: formulation and evaluation. Powder Technol. 2012;221:375–82.
14. Dudhipala N, Janga KY, Gorre T. Comparative study of nisoldipine-loaded nanostructured lipid carriers and solid lipid nanoparticles for oral delivery: preparation, characterization, permeation and pharmacokinetic evaluation. Artif Cells Nanomed Biotechnol. Taylor & Francis. 2018;46:616–25.
15. Krstić M, Medarević \DJor\dje, \DJuriš J, Ibrić S. Self-nanoemulsifying drug delivery systems (SNEDDS) and self-microemulsifying drug delivery systems (SMEDDS) as lipid nanocarriers for improving dissolution rate and bioavailability of poorly soluble drugs. Lipid nanocarriers for drug targeting. Elsevier; 2018. p. 473–508.
16. Cole ET, Cadé D, Benameur H. Challenges and opportunities in the encapsulation of liquid and semi-solid formulations into capsules for oral administration. Adv Drug Deliv Rev. Elsevier. 2008;60:747–56.
17. Chen F-J, Etzler FM, Ubben J, Birch A, Zhong L, Schwabe R, et al. Effects of lipophilic components on the compatibility of lipid-based formulations with hard gelatin capsules. J Pharm Sci Elsevier. 2010;99:128–41.
18. Agarwal V, Siddiqui A, Ali H, Nazzal S. Dissolution and powder flow characterization of solid self-emulsified drug delivery system (SEDDS). Int J Pharm. 2009;366:44–52.
19. Chauhan B, Shimpi S, Paradkar A. Preparation and characterization of etoricoxib solid dispersions using lipid carriers by spray drying technique. AAPS PharmSciTech. Springer. 2005;6:E405–9.

20. Franzé S, Selmin F, Samaritani E, Minghetti P, Cilurzo F. Lyophilization of liposomal formulations: still necessary, still challenging. Pharmaceutics. Multidisciplinary Digital Publishing Institute. 2018;10:139.
21. Kamal MM, Salawi A, Lam M, Nokhodchi A, Abu-Fayyad A, El Sayed KA, *et al*. Development and characterization of curcumin-loaded solid self-emulsifying drug delivery system (SEDDS) by spray drying using Soluplus® as solid carrier. Powder Technol. Elsevier. 2020;369:137–45.
22. Silva LAD, Almeida SL, Alonso EC, Rocha PB, Martins FT, Freitas LA, *et al*. Preparation of a solid self-microemulsifying drug delivery system by hot-melt extrusion. Int J Pharm Elsevier. 2018;541:1–10.
23. Thipsay P. Application of quality by design and process analytical technology towards hot-melt extrusion processes. 2019;
24. Batra A, Desai D, Serajuddin ATM. Investigating the use of polymeric binders in twin screw melt granulation process for improving compactibility of drugs. J Pharm Sci. 2017;106:140–50.
25. Shanmugam S. Granulation techniques and technologies: recent progresses. BioImpacts: BI. Tabriz University of Medical Sciences; 2015;5:55.
26. Lee DR, Kim YH, Park KW, Ho MJ, Jung HJ, Cho HR, *et al*. Fujicalin®-based solid supersaturable self-emulsifying drug delivery system (S-SEDDS) of tacrolimus for enhanced dissolution rate and oral absorption. J Pharm Investig. Springer. 2015;45:651–8.
27. Gumaste SG, Pawlak SA, Dalrymple DM, Nider CJ, Trombetta LD, Serajuddin AT. Development of solid SEDDS, IV: effect of adsorbed lipid and surfactant on tableting properties and surface structures of different silicates. Pharm Res. 2013;30:3170–85.
28. Gumaste SG, Dalrymple DM, Serajuddin AT. Development of solid SEDDS, V: compaction and drug release properties of tablets prepared by adsorbing lipid-based formulations onto Neusilin® US2. Pharm Res. 2013;30:3186–99.
29. Van Speybroeck M, Williams HD, Nguyen T-H, Anby MU, Porter CJ, Augustijns P. Incomplete desorption of liquid excipients reduces the in vitro and in vivo performance of self-emulsifying drug delivery systems solidified by adsorption onto an inorganic mesoporous carrier. Mol Pharm. 2012;9:2750–60.
30. Fuji Chemical Industry Co., Ltd. | APIs & Pharmaceuticals [Internet]. [cited 2020 Jan 14]. Available from: http://www.fujichemical.co.jp/english/medical/medicine/neusilin/index.html.
31. Mellaerts R, Mols R, Jammaer JA, Aerts CA, Annaert P, Van Humbeeck J, *et al*. Increasing the oral bioavailability of the poorly water soluble drug itraconazole with ordered mesoporous silica. European Journal of Pharmaceutics and Biopharmaceutics. Elsevier. 2008;69:223–30.
32. Vallet-Regí M, Ruiz-González L, Izquierdo-Barba I, González-Calbet JM. Revisiting silica based ordered mesoporous materials: medical applications. J Mater Chem. Royal Society of Chemistry. 2006;16:26–31.
33. Cha K-H, Cho K-J, Kim M-S, Kim J-S, Park HJ, Park J, *et al*. Enhancement of the dissolution rate and bioavailability of fenofibrate by a melt-adsorption method using supercritical carbon dioxide. Int J Nanomedicine. 2012;7:5565–75.
34. Jadhav NR, Irny PV, Patil US. Solid state behavior of progesterone and its release from Neusilin US2 based liquisolid compacts. J Drug Deliv Sci Technol Elsevier. 2017;38:97–106.
35. Bhagwat Durgacharan A, D'Souza JI. Development of solid self micro emulsifying drug delivery system with neusilin US2 for enhanced dissolution rate of telmisartan. Int J Drug Dev Res. 2012;4:398–407.
36. Kallakunta VR, Eedara BB, Jukanti R, Ajmeera RK, Bandari S. A Gelucire 44/14 and labrasol based solid self emulsifying drug delivery system: formulation and evaluation. J Pharm Investig. Springer. 2013;43:185–96.
37. Gupta MK, Vanwert A, Bogner RH. Formation of physically stable amorphous drugs by milling with Neusilin. J Pharm Sci. 2003;92:536–51.
38. Maclean J, Medina C, Daurio D, Alvarez-Nunez F, Jona J, Munson E, *et al*. Manufacture and performance evaluation of a stable amorphous complex of an acidic drug molecule and neusilin. J Pharm Sci. 2011;100:3332–44.
39. Bahl D, Bogner RH. Amorphization of indomethacin by co-grinding with Neusilin US2: amorphization kinetics, physical stability and mechanism. Pharm Res. 2006;23:2317–25.
40. Panigrahi KC, Patra CN, Jena GK, Ghose D, Jena J, Panda SK, *et al*. Gelucire: a versatile polymer for modified release drug delivery system. Futur J Pharm Sci. Elsevier. 2018;4:102–8.
41. Shin DJ, Chae BR, Goo YT, Yoon HY, Kim CH, Sohn SI, *et al*. Improved dissolution and Oral bioavailability of valsartan using a solidified Supersaturable self-microemulsifying drug delivery system containing Gelucire® 44/14. Pharmaceutics. Multidisciplinary Digital Publishing Institute. 2019;11:58.
42. Shimpi S, Chauhan B, Mahadik KR, Paradkar A. Preparation and evaluation of diltiazem hydrochloride-Gelucire 43/01 floating granules prepared by melt granulation. AAPS PharmSciTech. Springer. 2004;5:51–6.
43. Jain SK, Gupta A. Development of Gelucire 43/01 beads of metformin hydrochloride for floating delivery. AAPS PharmSciTech. Springer. 2009;10:1128.
44. Juarez-Soberanez D, Villafuerte-Robles L. Gelucire 39/01 as excipient for gastroretentive metronidazole sustained delivery. Int J Pharm Pharm Sci. 2011;3(Suppl 2):86–91.
45. Connors KA, Higuchi T. Phase solubility techniques. Adv Anal Chem Instrum. 1965;4:117–212.
46. USP. United States Pharmacopeia, 43rd revision. Rockville, MD: USP Convention, Inc; 2020:1833
47. Williams HD, Van Speybroeck M, Augustijns P, Porter CJ. Lipid-based formulations solidified via adsorption onto the mesoporous carrier Neusilin® US2: Effect of drug type and formulation composition on in vitro pharmaceutical performance. J Pharm Sci. 2014;103:1734–46.
48. DiNunzio JC, Schilling SU, Coney AW, Hughey JR, Kaneko N, McGinity JW. Use of highly compressible Ceolus™ microcrystalline cellulose for improved dosage form properties containing a hydrophilic solid dispersion. Drug Dev Ind Pharm. Taylor & Francis. 2012;38:180–9.
49. Kucera SU, DiNunzio JC, Kaneko N, McGinity JW. Evaluation of Ceolus™ microcrystalline cellulose grades for the direct compression of enteric-coated pellets. Drug Dev Ind Pharm. Taylor & Francis. 2012;38:341–50.
50. Kallakunta VR, Patil H, Tiwari R, Ye X, Upadhye S, Vladyka RS, *et al*. Exploratory studies in heat-assisted continuous twin-screw dry granulation: a novel alternative technique to conventional dry granulation. Int J Pharm. 2019;555:380–93.
51. Carr RL. Evaluating flow properties of solids. 1965;
52. Kallakunta VR, Sarabu S, Bandari S, Batra A, Bi V, Durig T, et al. Stable amorphous solid dispersions of fenofibrate using hot melt extrusion technology: effect of formulation and process parameters for a low glass transition temperature drug. J Drug Deliv Sci Technol. 2019;58:101395.
53. Damian F, Blaton N, Naesens L, Balzarini J, Kinget R, Augustijns P, *et al*. Physicochemical characterization of solid dispersions of the antiviral agent UC-781 with polyethylene glycol 6000 and Gelucire 44/14. Eur J Pharm Sci. Elsevier. 2000;10:311–22.
54. Karataş A, Yüksel N, Baykara T. Improved solubility and dissolution rate of piroxicam using gelucire 44/14 and labrasol. Il Farmaco. Elsevier; 2005;60:777–82.
55. Ganesh M. Design and optimization of rivaroxaban lipid solid dispersion for dissolution enhancement using statistical experimental design. Asian Journal of Pharmaceutics (AJP): Free full text articles from Asian J Pharm. 2016;10.
56. Le T-T, Elzhry Elyafi AK, Mohammed AR, Al-Khattawi A. Delivery of poorly soluble drugs via mesoporous silica: Impact of drug overloading on release and thermal profiles. Pharmaceutics. Multidisciplinary Digital Publishing Institute. 2019;11:269.
57. Fraser Steele D, Edge S, Tobyn MJ, Christian Moreton R, Staniforth JN. Adsorption of an amine drug onto microcrystalline cellulose and silicified microcrystalline cellulose samples. Drug Dev Ind Pharm. Taylor & Francis. 2003;29:475–87.
58. Zhang F. Physicochemical properties and mechanisms of drug release from melt-extruded granules consisting of

chlorpheniramine maleate and Eudragit FS. Drug Dev Ind Pharm. Taylor & Francis. 2016;42:563–71.
59. Ige PP, Baria RK, Gattani SG. Fabrication of fenofibrate nanocrystals by probe sonication method for enhancement of dissolution rate and oral bioavailability. Colloids Surf B: Biointerfaces. 2013;108:366–73.
60. Karolewicz B, Gajda M, Pluta J, Górniak A. Dissolution study and thermal analysis of fenofibrate–Pluronic F127 solid dispersions. J Therm Anal Calorim. 2016;125:751–7.
61. Aldosari BNA. Development and evaluation of self-nanoemulsifying drug delivery systems for oral delivery of indomethacin [PhD Thesis]. UCL (University College London); 2018.
62. McCormick D. Evolutions in direct compression. Pharm Technol. 2005;17:52–62.
63. Pitt KG, Heasley MG. Determination of the tensile strength of elongated tablets. Powder Technol. 2013;238:169–75.
64. Bala R, Khanna S, Pawar PK. Formulation and optimization of fast dissolving intraoral drug delivery system for clobazam using response surface methodology. J Adv Pharm Technol Res. Wolters Kluwer–Medknow Publications. 2013;4:151.
65. Ferrari F, Bertoni M, Bonferoni MC, Rossi S, Caramella C, Nyström C. Investigation on bonding and disintegration properties of pharmaceutical materials. International journal of pharmaceutics. Elsevier. 1996;136:71–9.
66. Mostafa HF, Ibrahim MA, Sakr A. Development and optimization of dextromethorphan hydrobromide oral disintegrating tablets: effect of formulation and process variables. Pharm Dev Technol. Taylor & Francis. 2013;18:454–63.